UNIVERSITÉ DE GENÈVE

SCHOLA GENEVENSIS MDLIX

A TIME EXPANSION CHAMBER AS A VERTEX DETECTOR

H.Anderhub[6], H.Anders[8], S.Ansari[7], A.Boehm[1], M.Bourquin[5], J.Burger[4]
M.Chen[4], V.Commichau[1], M.Deutschmann[1], M.Dhina[4], K.J.Draheim[1]
J.Fehlmann[6], D.Fong[4], U.Gessner[1], K.Hangarter[1], R.Hausammann[5]
U.Herten[1], H.Hofer[6], K.Hofmann[1], M.M.Ilyas[4], B.Krause[1], R.Leiste[10]
Q.Z.Li[6], D.Linnhoefer[1], X.Lue[6], S.Masson[1], M.Nusbaumer[5], H.Nierobisch[1]
M.Pohl[6], R.R.Rau[2], D.Ren[6], E.Roderburg[9], M.Rohde[3], J.Schug[1], B.Stoehr[6]
S.C.C.Ting[4], M.Tonutti[1], G.Viertel[6], S.X.Wu[4], M.F.Wyne[7], B.Wyslouch[4]

Presented by R.Hausammann

3rd Pisa Meeting on Advanced Detectors

Castiglione della Pescaia, Italy, June 2 - 7, 1986

UGVA-DPNC 1986/10-115

1) Rhein.-Westf. Technische Hochschule, III. Physik. Inst.
Physikzentrum, 5100 Aachen, Federal Republic of Germany
2) Brookhaven National Laboratory (BNL), Upton, New York, USA
3) Deutsches Elektronen-Synchrotron (DESY), 2000 Hamburg
Federal Republic of Germany
4) Massachusetts Institute of Technology (MIT), Cambridge, USA
5) University of Geneva, DPNC, 1211 Geneva, Switzerland
6) Eidg. Technische Hochschule, Inst. f. Hochenergiephysik
8093 Zurich, Switzerland
7) Pakistan Atomic Energy Commission, Islamabad, Pakistan
8) European Organization for Nuclear Research (CERN)
1211 Geneva, Switzerland
9) Univ. Gesamthochschule Siegen, Fachbereich 7 - Physik
5900 Siegen, Federal Republic of Germany
10) Institut fuer Hochenergiephysik der AdW der DDR
1615 Zeuthen, German Democratic Republic

Abstract

A high-resolution drift chamber based on the time expansion principle has been built as a vertex detector for the Mark J experiment at DESY. The chamber design and the associated control and readout system are described. Results on chamber performance obtained from test beam measurements and first results from running at PETRA are reported.

1. Introduction

The lifetime measurement of heavy flavored particles in high-energy collisions requires the precise determination of the so-called impact parameter [1] for secondary particle tracks. As this quantity is around 100 microns, vertex detectors with resolutions better than this are asked for. The experiment L3 for LEP [2] has opted for a high-resolution drift chamber based on the time expansion principle (TEC) [3]. The TEC aims to reach the ultimate drift chamber resolution by means of the following features:

- low-field drift region (drift velocity around 5 microns/nsec) separated from high-field detection region
- analog shaping of anode signal to cancel ion tail
- 100 MHz flash-ADC to digitize anode pulse shape in order to apply a drift time determination by center of gravity method
- drift chamber gas with lowest possible diffusion (cool gas) and small Lorentz angle

First prototype tests in 1983 [4] showed promising results with single and double-track resolutions of around 30 and 300 microns, respectively. In order to test the novel TEC technique under realistic conditions, a small cylindrical vertex detector has been built for the experiment Mark J [5] at DESY, although the relative small drift distances available (less than 27 mm) do not make optimal use of the merits of the TEC. The chamber was successfully tested in beam prior to installation into the Mark J detector in December 1985.

2. The Mark J TEC

By reducing the diameter of the original Mark J beam pipe from 190 mm to 100 mm and the construction of a new set of the 2600 z-layer tubes [6], the installation of the new vertex detector was accomplished with minimal change to the existing apparatus.

2.1 Chamber design

A schematic axial view of the Mark J vertex chamber is given in figure 1. The TEC is built on the fully supporting beam pipe which consists of 1.4 mm carbonfiber-epoxy and an inner coating of stainless steel, 0.2 mm thick over a length of 400 mm in the center, followed by 4 mm thick extensions towards the chamber endflanges. The two circular endplates, 24 cm in diameter, are also made of stainless steel and glued at a distance of 60 cm onto the beam pipe, electrically isolated by 300 microns of ceramic. The sensitive volume of the chamber is subdivided into 12 drift segments with a 4 mm wide detection gap in the center, inclined by 4 deg in order to resolve the left-right ambiguity. 552 feedthroughs are mounted into the endplates in which the 80 microns molybdenum fieldshaping wires are strung. In addition, 12*2 slits (2mm wide and 20 mm long) at the positions of the detection gaps provide for precision mounting of the detection gap holders. Each gap holder, made of stainless steel 54.4 mm long and 4 mm wide, has a series of precision grooves on both sides to which 77 100 microns molybdenum grid wires are attached with a spacing of 0.6 mm. A 0.3 mm thick ceramic plate is glued onto the gap holders towards the sensitive chamber volume in order to hold the 2*7 anode wires, made of 20 microns of tungsten, interleaved with 2*8 100 microns molybdenum focus wires at a relative spacing of 1.2 mm. The overall absolute mechanical accuracy is less than 10 microns. The load of 8 kN from the wire tension is entirely supported by the beam pipe. The chamber is closed from the outside by a 3 mm thick aluminum cylinder slid over the endplates and fixed with air-tight rings screwed to the outer side of the endflanges. Table 1 and 2 list the chamber parameters. More details, in particular about the construction procedure, can be found in reference [7].

Due to a default in the fabrication process of the beam pipe by industry, the 0.2 mm steel inliner collapsed when exposed to both outer pressure of 2 bars and vacuum inside. It could be removed and replaced by a 2 mm thick aluminum tube just before installation into the Mark J detector. By means of an electro-mechanical resonance technique it was verified that the proper tension of the anode wires was not affected by this incident.

2.2 Gas system

The chamber is operated with a gas mixture of 80% CO_2 and 20% $i\text{-}C_4H_{10}$ at a pressure of 1.9 bar. The mixture chosen has the required low longitudinal diffusion, crucial to attain the high resolution, and, although not important for Mark J, a small Lorentz angle at TEC operating conditions [8]. In addition, the oxygen equivalent impurities have to be kept below the ppm level in order to avoid electron attachment during drift. And last not least, temperature, pressure and gas composition have to be controlled at the per mille level as the drift velocity varies linearly with these quantities in our range of operation. The above conditions delimited the gas system developed for this experiment [9], see figure 2. The gas in the closed-loop circuit is regularly pumped through "OXYSORB" in bypass to allow a maximum flow of 60 lt/min . This keeps the oxygen impurities below 0.1 ppm and the water content to less than 1 ppm. To avoid other impurities, only copper tubing is used in the system to the chamber. The gas pressure within the chamber is stabilized within 1 mbar with respect to a fixed pressure of a closed reference volume. Various instruments monitor the gas composition: BINOS measures the isobutane and PANAMETRICS the water content and a gas chromatograph is used for periodical analysis. The entire system is controlled by a dedicated computer. In addition, during data acquisition the temperature and pressure sensors are read out by the host computer for each event and written to tape.

2.3 High voltage system

The high voltage values to be applied in order to render the drift field as homogeneous as possible has been optimized beforehand by computer [10]. Possibility for individual final tuning is provided for all the fieldshaping wires (except for the cathodes which are on fixed resistor chains), the inner and outer potential and most of the anodes. In addition all supplies are repeated for the 12 segments. This individuality proved to be useful for temporarily disconnecting hot wires. This is accomplished via a special distribution panel from which 450 cables are sent to the chamber. It is powered from 3 LRS HV-4032 mainframes. They are interfaced via CAMAC to the data acquisition host computer (see next paragraph) which runs a comprehensive high voltage control program [11]. The actual high voltage settings and currents are read out periodically during data acquisition and recorded.

2.4 Readout

The anodes, being at a potential of about 3000 volts, are capacitively coupled to fast low-noise, current-sensitive, low-power preamplifiers of the type MSD2 [12]. Four channels are mounted on one card in thick-film hybrid circuit technology. 48 cards for the 168 anodes are directly attached to one endflange of the chamber in order to minimize cable length. The signals from the preamps are sent over 30 m of coaxial cables to Cable Equalizer Amplifier [13] modules outside the confined zone of the detector. They reshape and amplify the attenuated signals and drive them over another 30 m to signal amplifier-shapers [4,14] located in the counting room which cancel the ion tail of the drift signal.

Each output channel of the shapers is then fed into a 100 MHz 6-bit FADC housed in a 1-U CAMAC module [15]. They sample the incoming signal at 10 nsec intervals and store the digitized amplitudes into a fast 1 kbyte deep ECL RAM. To each FADC a Data Reduction Processor (DRP) is associated. This is a 1-U CAMAC module [15] equipped with a TMS 9900 CPU, 16 kbyte ROM and 16 kbyte RAM for program storage and data buffering and a DMA port for fast data transfer from the FADC. Its function is to reduce the prohibitive large amount of raw data. Four different data reduction modes can be selected:

1. "Raw Data" : no data reduction

2. "Compressed": data in selectable regions are compressed

3. "Differential Threshold": data above threshold and additional channels before and after the signal are compressed

4. "Cluster Parameter": data are reduced to 11 parameters (e.g. peak amplitude, integral, width, baseline) for each signal cluster found

In order to preserve as much information as possible for subsequent off-line analysis, compute mode number 3 has been chosen by which an overall data reduction factor of typically 17 is achieved.

2*6 anodes are equipped with digital readout electronics for each of the 12 chamber segments. The readout of the total of 144 DRP modules distributed over 16 CAMAC crates is accomplished with a VAX-11/750 computer configuration assisted by 16 intelligent CAMAC auxiliary crate controllers (ACC) [16] based on Fairchild's 9445 microprocessor as event-builders for each crate, see figure 3. They allow the relative slow readout of all crates in parallel without intervention of the VAX which is only interrupted after all ACC's have collected the data from their crate. The readout from the ACC's memories proceeds over fast DMA transfers which results in a minimal data acquisition load for the VAX of less than 15% for a typical event rate of 8 kbyte at 2 Hz. Ample CPU time is therefore available for data monitoring and event display. The TEC readout is independent from the Mark J system except for the trigger to start digitization. To ensure safe merging of data recorded from the two independent systems, a 15-bit event number and a trigger bit generated on Mark J are sent to the TEC system and attached to each event.

3. Measurements in test beam

A single segment prototype chamber and two opposite segments of the Mark J TEC have been exposed to a beam of 5 GeV/c electrons at DESY prior to installation into the detector. The following summarizes the main results from test data analysis. More details can be found in references [17], [18] and [7].

3.1 Calibration

The drifttime-space relationship relates the measured drifttime to absolute space-points over the drift velocity:

$$x_i = v_i * t_i = v_i * (t_{COG_i} - t_{M_i} - t_{GR_i} + t_A)$$

$$i = 1, \ldots, 14 \quad \text{anode number}$$

t_{COG} is the drifttime of the track signal determined by a center of gravity method with an accuracy of well below 1 nsec owing to the fast FADC. t_M is the time reference obtained from the time-marker signal injected capacitively over the focus wires at a well-defined time after the digitization start signal, derived from the trigger. It also has an accuracy of much better than 1 nsec. t_{GR} is the drifttime which corresponds to the transition from the low drift field to the high detection field near the grid. t_A is the average time-marker position and is introduced to redefine the drifttime zero point.

Drift velocity v and grid position t_{GR} were measured for each anode with the help of two silicon microstrip detectors placed outside the chamber. With a pitch of 50 microns they determined the track position to better than 15 microns. This excellent resolution, however, was degraded considerably inside the chamber due to multiple scattering in the outer chamber walls. Accumulation of sufficient statistics could make up for this. Figure 4 shows the results for the drift velocities. They could be determined within 3 ‰. Small deviations of less than 5 ‰ from a common mean drift velocity is the result of excellent field homogeneity owing to tight tolerances in construction. The outer anodes 1 and 14 deviate more due to edge effects. The present values are the basis for the Mark J TEC calibration after correction for different temperature and pressure.

3.2 Resolution

The absolute drifttime-space relationship has been obtained by comparing track trajectories as measured by the chamber to the independent microstrip positions. In order to find the inner TEC resolution, distributions of residuals from straight track reconstructions within the chamber only have been accumulated. The width of the residual distribution gives an estimate for the intrinsic chamber resolution independent of calibration, up to a known geometry factor [4]. Figure 5 shows a typical example of the resolution measured as a function of drift length. Modeling the drift length dependence with a part caused by longitudinal diffusion and a constant contribution, the dependence can be fitted by

$$\sigma_i = \sqrt{A_i^2 x + B^2} \qquad i = 1,\ldots,14 \qquad (1)$$

Typical values obtained for A and B are indicated in figure 5. In the average over all inner anodes measured, the resolution is 35.5 microns at 1 cm drift length and remains below 50 microns over the homogeneous drift region.

The dependence of the resolution on the azimuthal angle is displayed in figure 6. The angle for tracks originating from the interaction point is limited to 19 deg.

For the determination of the chamber's resolution with regard to vertex reconstruction, the difference of offsets in the center obtained from the individual reconstruction in opposite segments of through-going tracks has been measured. Figure 7 displays the distribution of differences. The width measures the accuracy due to the inner resolution by which the impact parameter, a quantity employed in the determination of secondary vertices [1], can be reconstructed. Assuming both segments contribute equally, an error of 80 microns can be derived. The contribution from multiple scattering of 5 GeV/c electrons in the beam pipe (2.1 % radiation length), included in this measurement, is about 20 microns. This contribution becomes somewhat larger for secondaries in B-meson decays with momentums around 2.5 GeV/c. However, the use of a 1.5 mm beryllium pipe, initially considered but then abandoned for cost and time reasons, would be perfectly possible from mechanical stability and would make multiple scattering much smaller than the chamber reconstruction errors. This excellent vertex resolution demonstrates that the Mark J TEC is an instrument perfectly suited for the lifetime measurements of heavy flavored particles.

The double-track resolution, important for disentangling tracks in high-multiplicity events, has been studied in detail for data taken with the single segment prototype chamber. A value of 300 +- 50 microns has been obtained for a track separation at which 50 % of the tracks are correctly resolved [19].

3.3 Electron statistics

The length of the track sampled per anode is adjusted by varying the potential of the focus wires, presently at about the potential of the anodes. This sets the length to 1.2 mm in order to minimize the width of the electron arrival time distribution being part of B in equation (1), see also reference [4]. On the other hand, the diffusive part A improves with the number of electrons N_e generated, see equation (2) below. Based on measured values of A, N_e seems somewhat marginal and much lower than the expected number of about 20 electrons. For this reason test data have been examined regarding electron statistics.

The measured TEC resolution due to diffusion, the first term in equation (1), is related to the number of electrons generated and the single electron diffusion:

$$\sigma(x) = \sigma_0 \sqrt{x / N_e} \qquad (2)$$

We have determined σ_0 from the TEC signal widths. It corresponds to the gas diffusion constant and is in good agreement with calculated values, see references [18] and [7]. From this relation N_e can be estimated and one obtains 2.0 +- 0.5 electrons, far below the expected 20.

Another source of information on N_e is the dependence of the resolution on the azimuthal track angle φ to the anode plane. For angles different from zero the resolution becomes worse due to additional geometric broadening of the depth along the drift direction where the charge is created, see for example figure 6:

$$\sigma(\varphi) = (d / \sqrt{12}) \, tg\varphi \, (1 / \sqrt{N_e})$$

d is the sampling corridor width and $d*tg\varphi$ the longitudinal projection. Fitting the above relationship through measured points at 5 φ-angles between 0 and 21 deg for a drift distance around 1 cm, one obtains N_e = 3 +- 1 electrons, in agreement with the result above.

A third point of interest is the dependence of the measured resolution on the polar angle θ which has been studied in detail for the single segment prototype chamber. Figure 8 displays the measured points as a function of θ. The θ-dependence can be described again by the geometric projection of the sampled track, this time along the anode wire:

$$\sigma(\theta) = \sigma_0 \sqrt{\sin\theta} \quad 1 / \sqrt{N_e}$$

For angles θ < 90 deg, one expects an improvement of resolution with the larger number of electrons, proportional to the sampled track length. The points below the measured ones represent an extrapolation from 30 deg scaled with the squareroot of sin θ. One notes that the measured dependence leads to a resolution at 90 deg being lower than expected. This may be an indication of saturation effects when all the charge gets amplified at one point at the anode. At 90 deg one can read off a potential improvement in resolution of 10 microns if it is possible to tune the anode voltage such that the TEC can operate at 90 deg as well as at 30 deg. Further studies will investigate this behaviour.

4. First results from PETRA

After installation into the Mark J detector in December 1985, the chamber was run in with cosmic rays until February 1986 when PETRA beam came on. During the first few weeks a great effort was needed to get the background down to a level acceptable for stable TEC operation. This was achieved by a combination of beam tuning and improvement in the vacuum system. Then the chamber could be run in quite stable conditions at peak currents of 10 to 11 mA per beam.

Analysis of first data taken is in progress. Examples of reconstructed events are shown in figure 9 for a Bhabha and in figure 10 for a hadronic event. Note that the beam position is off-center horizontally by about 6 mm toward the ring outside. At this position the background was found to be minimal. To ensure good resolution of left-right ambiguity, however,a better centered beam was preferred in a later stage of the experiment. Figure 11 displays the single wire efficiency as measured with cosmic rays with values around 90 % for most of the wires. From the reconstructed tracks the inner chamber resolution was estimated. Figure 12 shows the distribution of residuals obtained from Bhabha events summed over drift distances and angles. An average resolution of 40 microns can be read off, as expected from test beam measurements. Figure 13 displays the resolution as a function of drift distance, estimated from the width of residual distributions. Again, as observed in test beam measurements, the values depart from the slowly increasing function for drift lengths close to the cathodes.

5. Conclusions

A small cylindrical vertex chamber based on the time expansion principle has been built for the experiment Mark J at DESY and successfully tested in beam. An average resolution of 35 microns has been measured at 1 cm drift distance. It increases only slowly with drift length and azimuthal angle. A resolution of less than 100 microns on the impact parameter demonstrates the potential of the chamber regarding lifetime measurements of heavy flavored particles. First results from data taken at PETRA show a single wire resolution of 40 microns averaged over drift distances and angles and are in agreement with test beam measurements.

We thank the team of Mark J for their support and patience while running the TEC in parallel, and the technicians of RWTH Aachen, CERN, DESY, EIR, ETH-Zurich and the University of Geneva for their invaluable assistance. The financial support by the Swiss National Foundation for Scientific Research and "Bundesministerium fuer Forschung und Technologie" is acknowledged.

References

1. S.Petrera,G.Romano, Nucl. Instr. Meth. 174(1980)61

2. L3 Technical Proposal, LEPC/83-5/P4, 1983, CERN, Geneva, Switzerland

3. A.H.Walenta, IEEE Nucl. Sci. NS-26, Nr. 1(1979)73

4. V.Commichau et al., Nucl. Instr. Meth. A235(1985)267

5. The Mark J Collaboration, Physics Reports 63(1980)339

6. A.Donat et al., Internal Report, IfH Zeuthen (1985)

7. H.Anderhub et al., A Time Expansion Chamber as a Vertex Dtector for the Experiment Mark J at DESY, Wire Chamber Conference, Vienna, 1986, to be published in Nucl. Instr. Meth. (1986)

8. U.Becker et al., Nucl. Instr. Meth. 214(1983)525

9. F.Beissel et al., Development of a Gas System for the Mark J TEC Detector, III. Phys. Inst. RWTH Aachen (1985)

10. J.Fehlmann, "WIRCHA": A Program Package to Simulate Drift Chambers, ETH-Zurich (1985)

11. J.Fehlmann et al., High Voltage System for the Mark J Vertex Detector, Internal Report, ETH-Zurich, IHP 85-7 (1985)

12. P.Jarron, M.Goyot, Nucl. Instr. Meth. 226(1984)156

13. H.Anders et al., CERN-DD 85-20 (1985)

14. J.A.Paradiso, Compilation of Data on the Current TEC Analog Electronics, ETH-Zurich (1983)

15. V.Commichau et al., Internal Report, III. Phys. Inst. RWTH Aachen (1984)

16. M.Bourquin et al., Nucl. Instr. Meth. A239(1985)562

17. F.Muheim, Diploma Work, ETH-Zurich, IHP 85-10 (1985)

18. B.Stoehr, Diploma Work, ETH-Zurich, IHP 86-04 (1986)

19. B.Wyslouch, Mark J Internal Note, 31 July 1985

Table Captions

1. Parameters of the Mark J TEC

2. Maximum drift length for anode wires

Figure Captions

1. Axial view of Mark J TEC

2. Block diagram of Mark J TEC gas system

3. Mark J TEC readout architecture

4. Deviation of measured drift velocities from mean <v> for inner anodes

5. Top: Deviation of track position measured from fitted track
   Middle: Measured spatial resolution as function of drift length
   Bottom: Beam profile from which measurements result

6. Dependence of resolution on azimuthal angle

7. Difference of offsets of independent reconstruction from opposite segments for through-going tracks

8. Resolution as function of polar angle compared with expected extrapolation from 30 deg

9. Example of reconstructed Bhabha event

10. Example of reconstructed hadronic event

11. Single wire efficiency from cosmic events

12. Residual distribution from Bhabha events, summed over drift distances and angles

13. Resolution as function of drift distance

Table 1: Parameters of the MARK J vertex chamber

inner diameter	100 mm
outer diameter	242 mm
sensitive wire length	576 mm
number of segments	12
number of sense wires per segment	14
total number of sense wires	168
spacing between anodes	2.4 mm
spacing between potential wires	2.54 mm
spacing between grid wires	0.6 mm
gas mixture	CO_2-i-C_4H_{10} (80 %-20 %)
pressure	1.9 bar
drift velocity	7 micron/ns

Table 2: Maximum drift length to the anode wires

ANODE =	SUBSEGMENT	
	BIG	SMALL
1 (R=60 mm)	19.5	13.3
2	20.0	14.1
3	20.5	14.9
4	21.0	15.7
5	21.5	16.5
6	22.0	17.3
7	22.5	18.1
8	24.5	22.6
9	25.0	23.4
10	25.5	24.2
11	26.0	25.0
12	26.5	25.8
13	27.0	26.6
14 (R=99 mm)	27.5	27.4

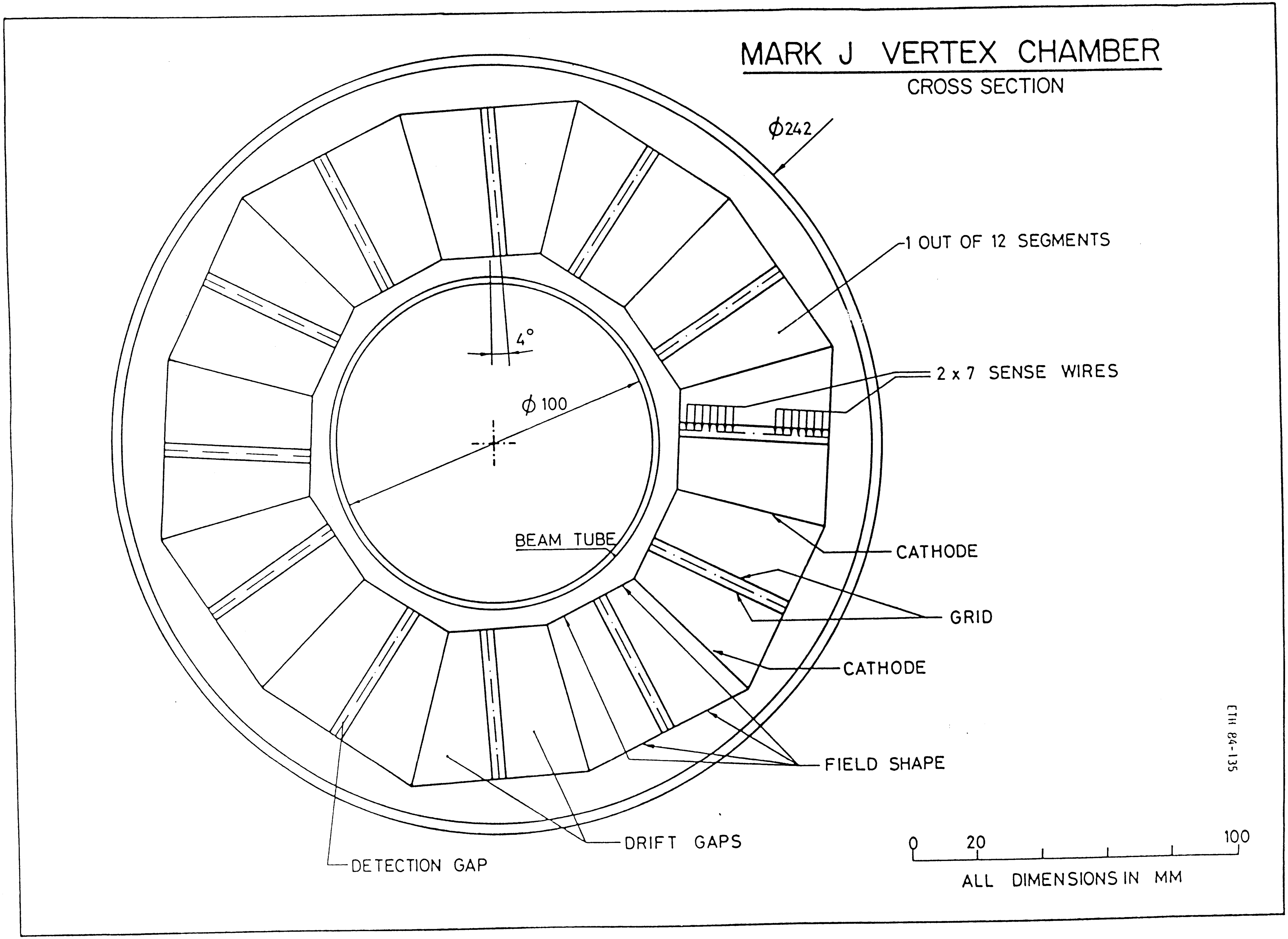
MARK J VERTEX CHAMBER
CROSS SECTION
ϕ242
1 OUT OF 12 SEGMENTS
4°
2 x 7 SENSE WIRES
ϕ 100
BEAM TUBE
CATHODE
GRID
CATHODE
FIELD SHAPE
ETH 84-135
DRIFT GAPS
DETECTION GAP
0
20
100
ALL DIMENSIONS IN MM

FIG. :

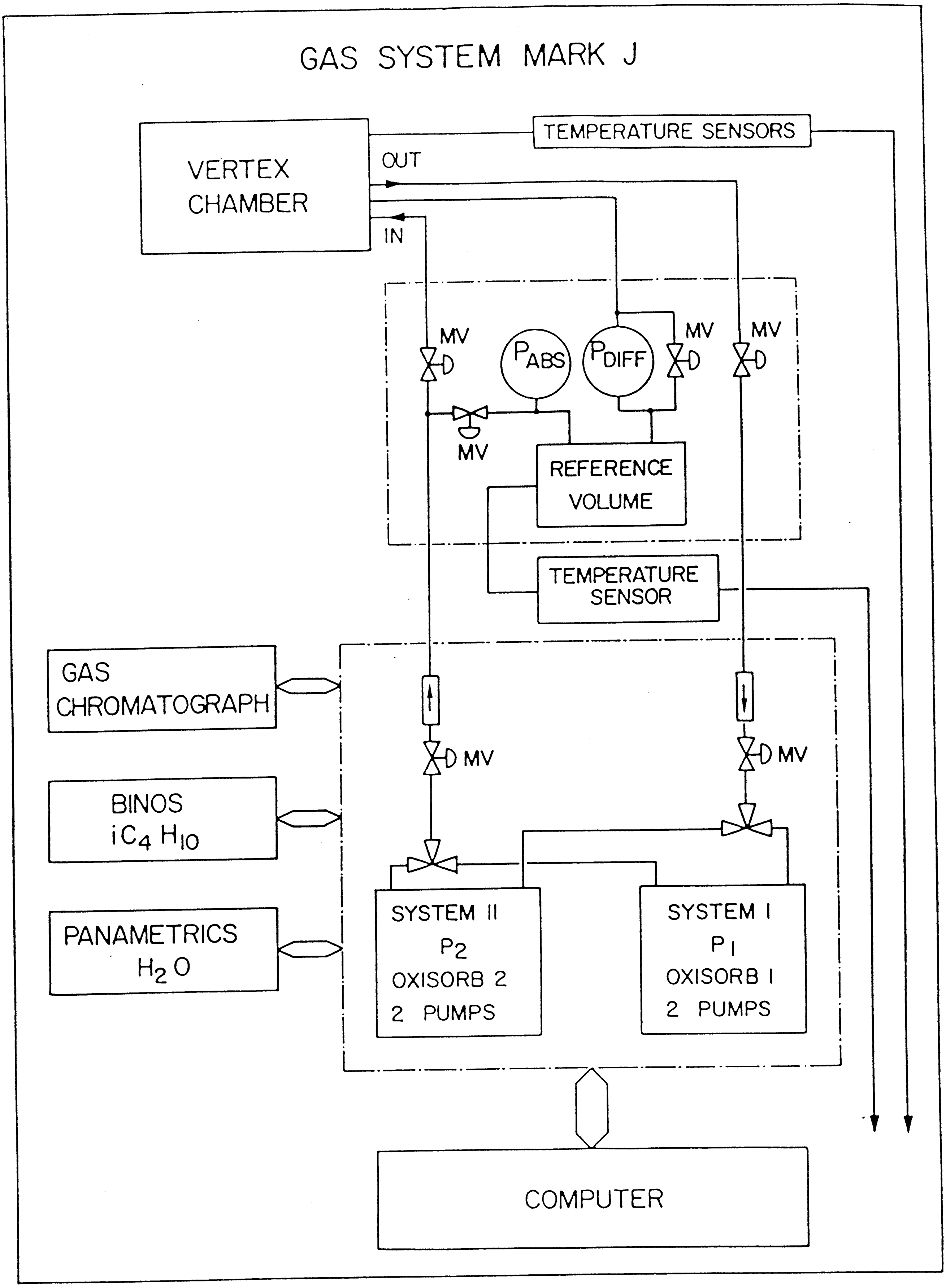
GAS SYSTEM MARK J
VERTEX CHAMBER
TEMPERATURE SENSORS
OUT
IN
MV
P_{ABS}
P_{DIFF}
MV
MV
MV
REFERENCE VOLUME
TEMPERATURE SENSOR
GAS CHROMATOGRAPH
BINOS
iC_4H_{10}
PANAMETRICS
H_2O
MV
MV
SYSTEM II
P_2
OXISORB 2
2 PUMPS
SYSTEM I
P_1
OXISORB 1
2 PUMPS
COMPUTER

FIG. 2

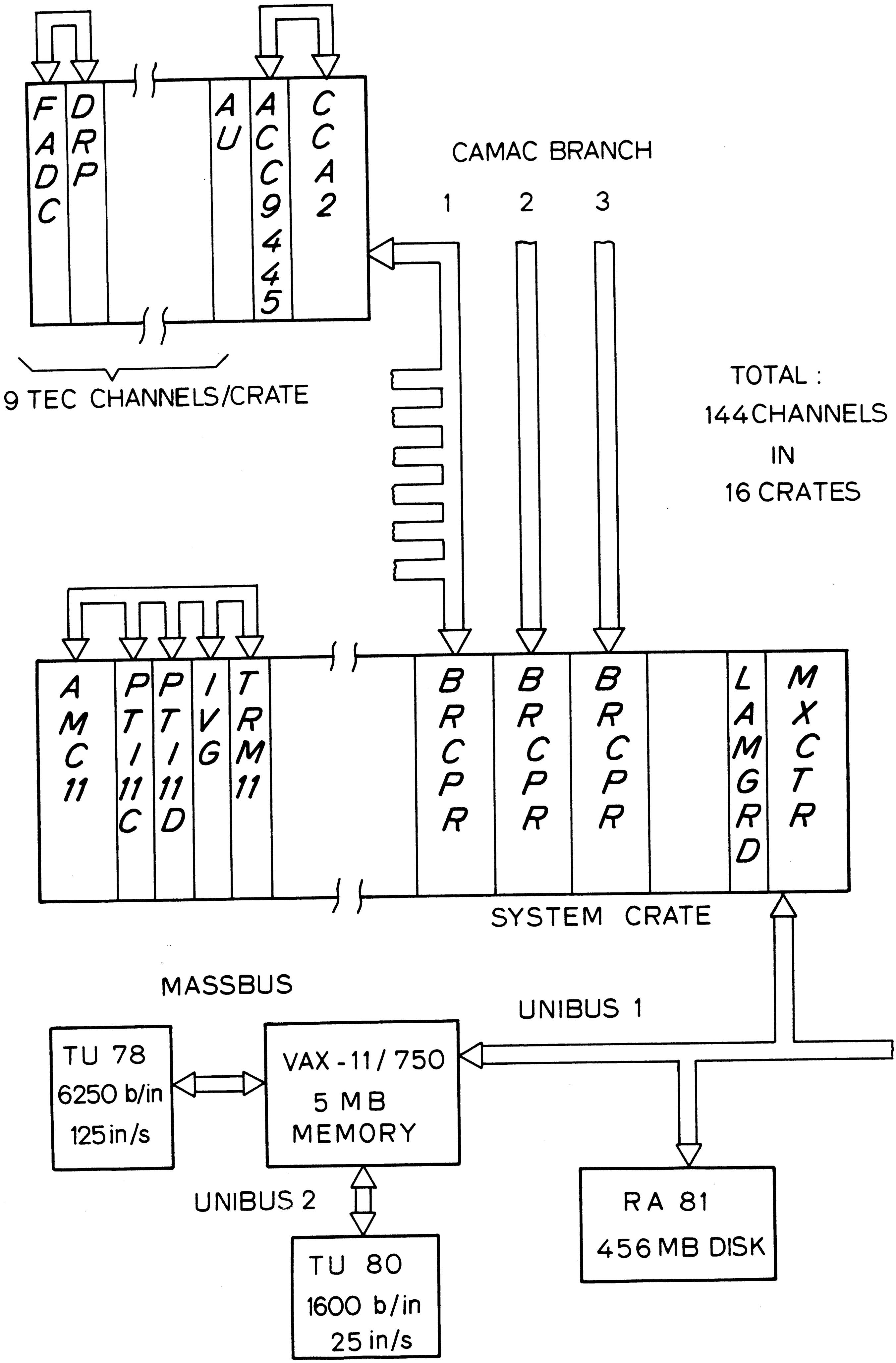
F A D C
D R P
A U
A C C 9 4 4 5
C C A 2
CAMAC BRANCH
1
2
3
9 TEC CHANNELS/CRATE
TOTAL :
144 CHANNELS
IN
16 CRATES
A M C 11
P T I 11 C
P T I 11 D
I V G
T R M 11
B R C P R
B R C P R
B R C P R
L A M G R D
M X C T R
SYSTEM CRATE
MASSBUS
UNIBUS 1
TU 78
6250 b/in
125 in/s
VAX - 11 / 750
5 MB
MEMORY
UNIBUS 2
RA 81
456 MB DISK
TU 80
1600 b/in
25 in/s

FIG. 3

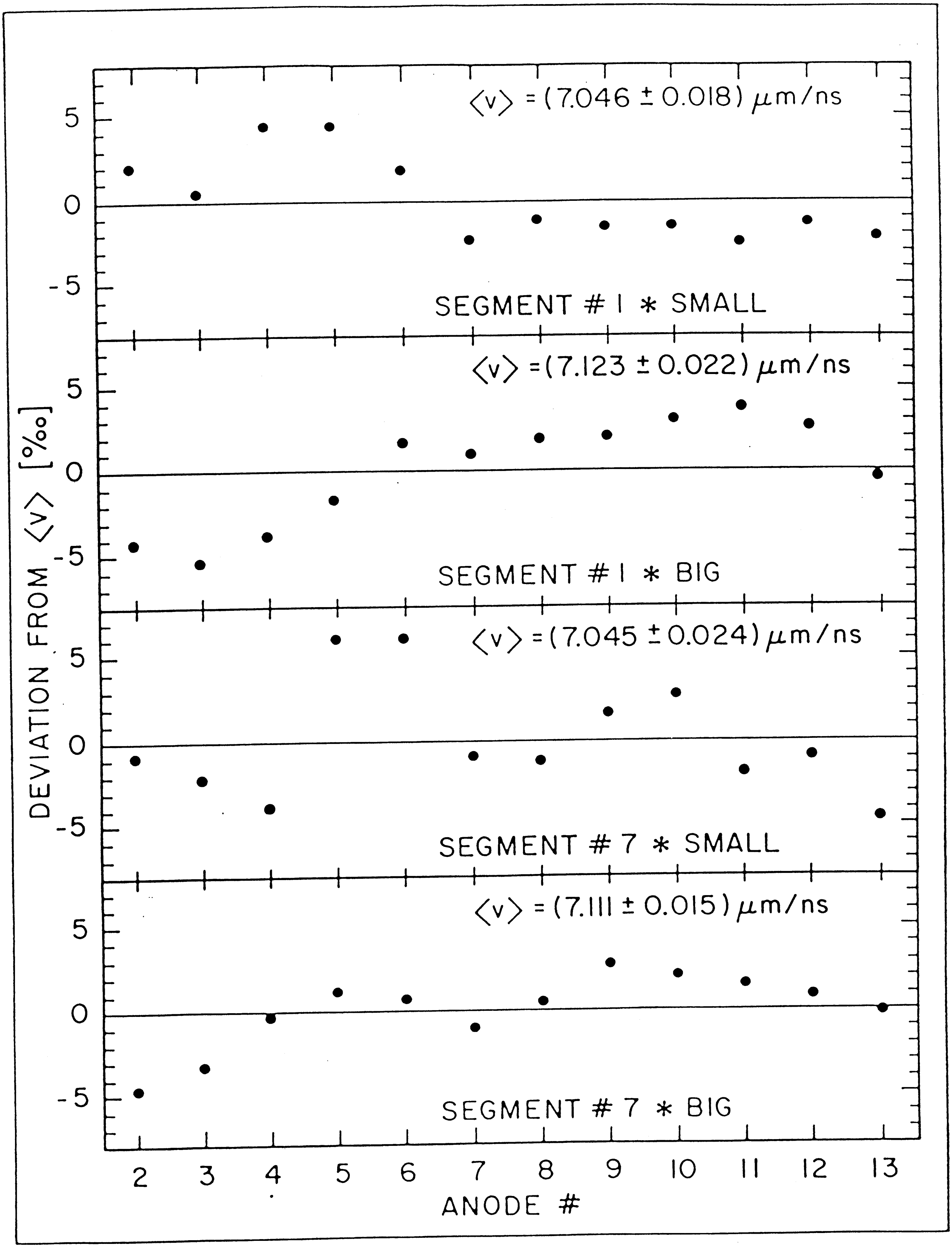

⟨v⟩ = (7.046 ± 0.018) μm/ns
SEGMENT # 1 * SMALL
⟨v⟩ = (7.123 ± 0.022) μm/ns
SEGMENT # 1 * BIG
⟨v⟩ = (7.045 ± 0.024) μm/ns
SEGMENT # 7 * SMALL
⟨v⟩ = (7.111 ± 0.015) μm/ns
SEGMENT # 7 * BIG
DEVIATION FROM ⟨v⟩ [‰]
5
0
-5
2
3
4
5
6
7
8
9
10
11
12
13
ANODE #

FIG. 4

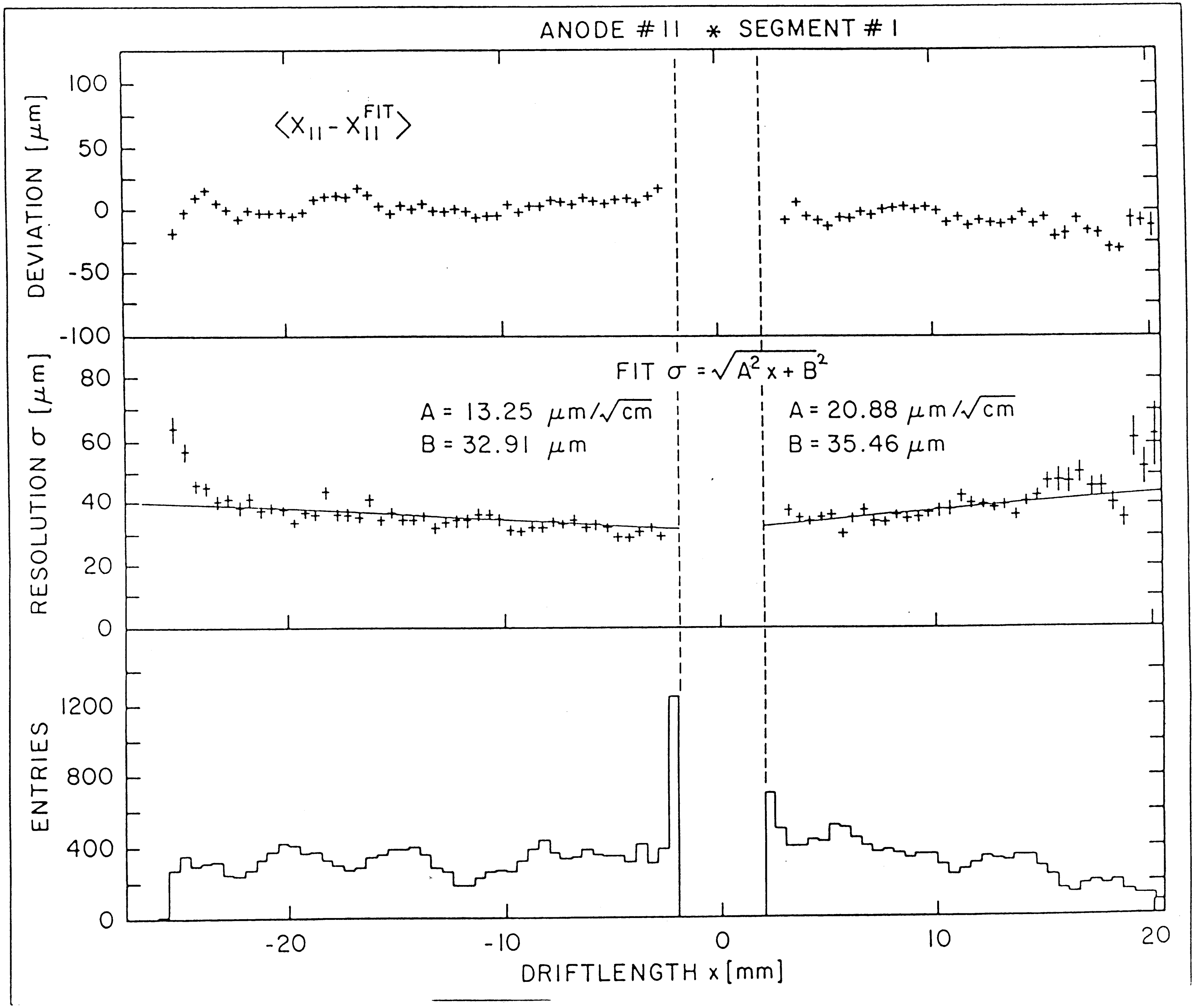

ANODE #11 * SEGMENT #1
⟨X11 - X11 FIT⟩
DEVIATION [μm]
100
50
0
-50
-100
FIT σ = √(A² x + B²)
A = 13.25 μm/√cm
B = 32.91 μm
A = 20.88 μm/√cm
B = 35.46 μm
RESOLUTION σ [μm]
80
60
40
20
0
ENTRIES
1200
800
400
0
-20
-10
0
10
20
DRIFTLENGTH x [mm]

FIG. 5

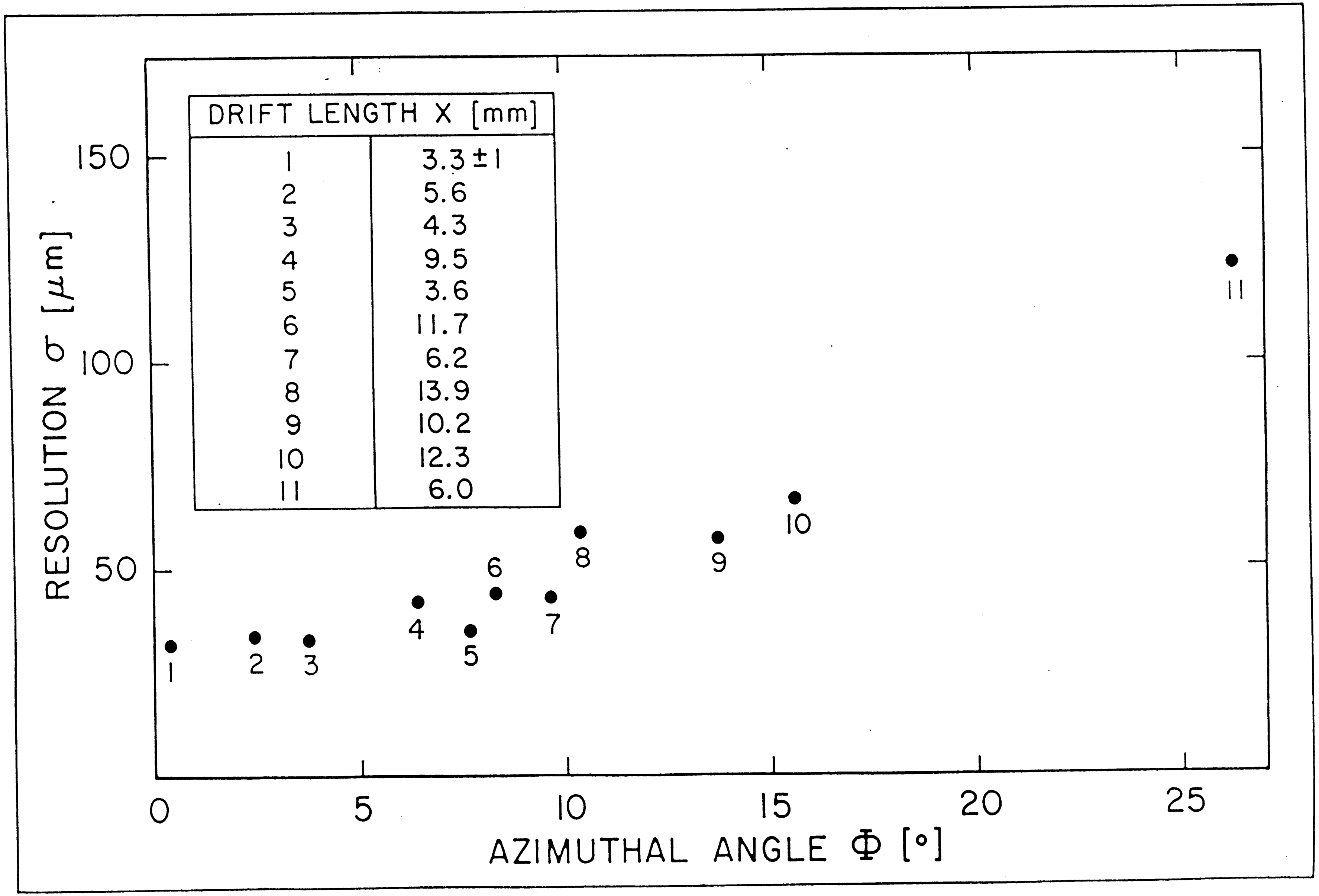

DRIFT LENGTH	X [mm]
1	3.3±1
2	5.6
3	4.3
4	9.5
5	3.6
6	11.7
7	6.2
8	13.9
9	10.2
10	12.3
11	6.0

FIG. 6

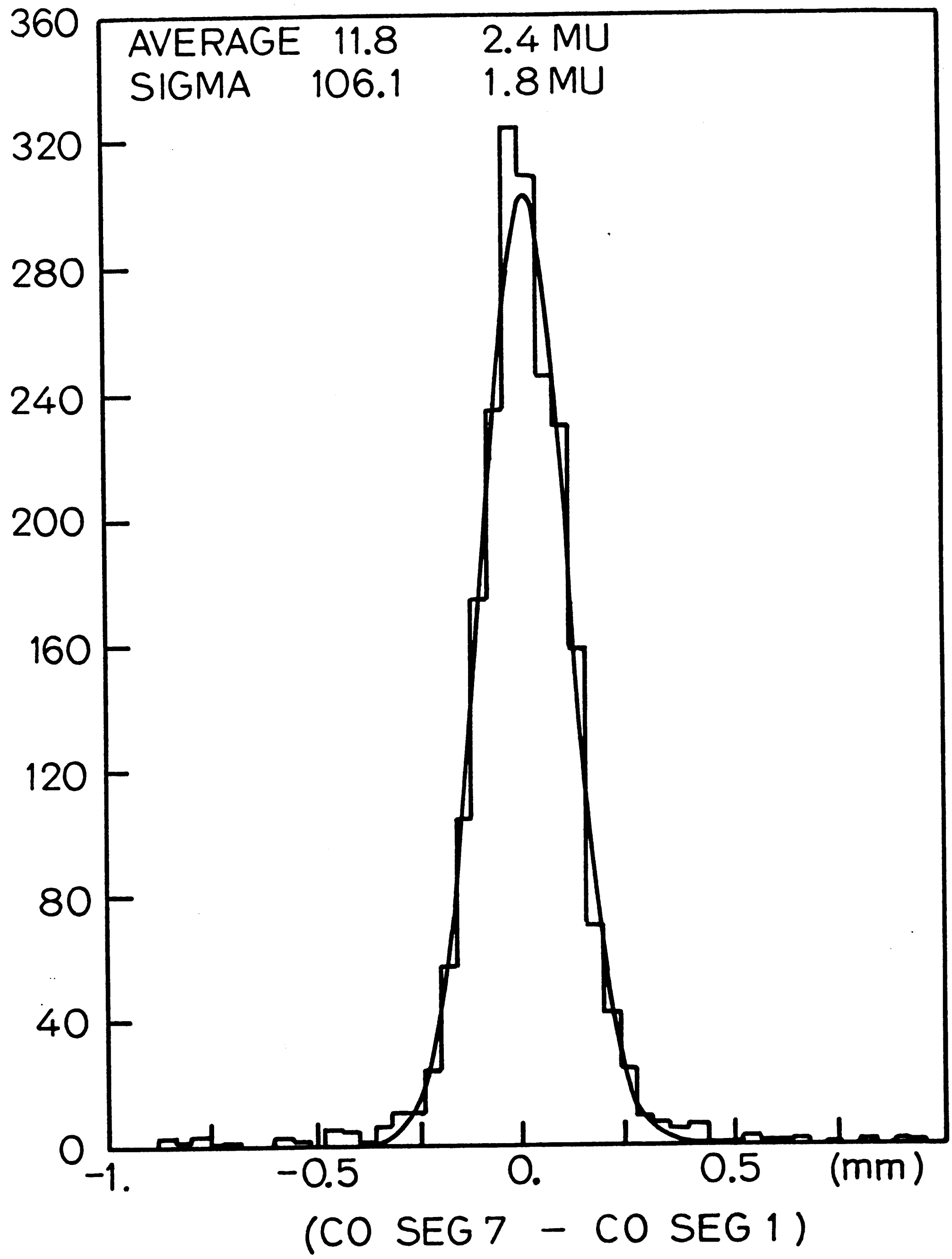
AVERAGE 11.8 2.4 MU
SIGMA 106.1 1.8 MU
360
320
280
240
200
160
120
80
40
0
-1.
-0.5
0.
0.5
(mm)
(CO SEG 7 - CO SEG 1)

FIG. 7

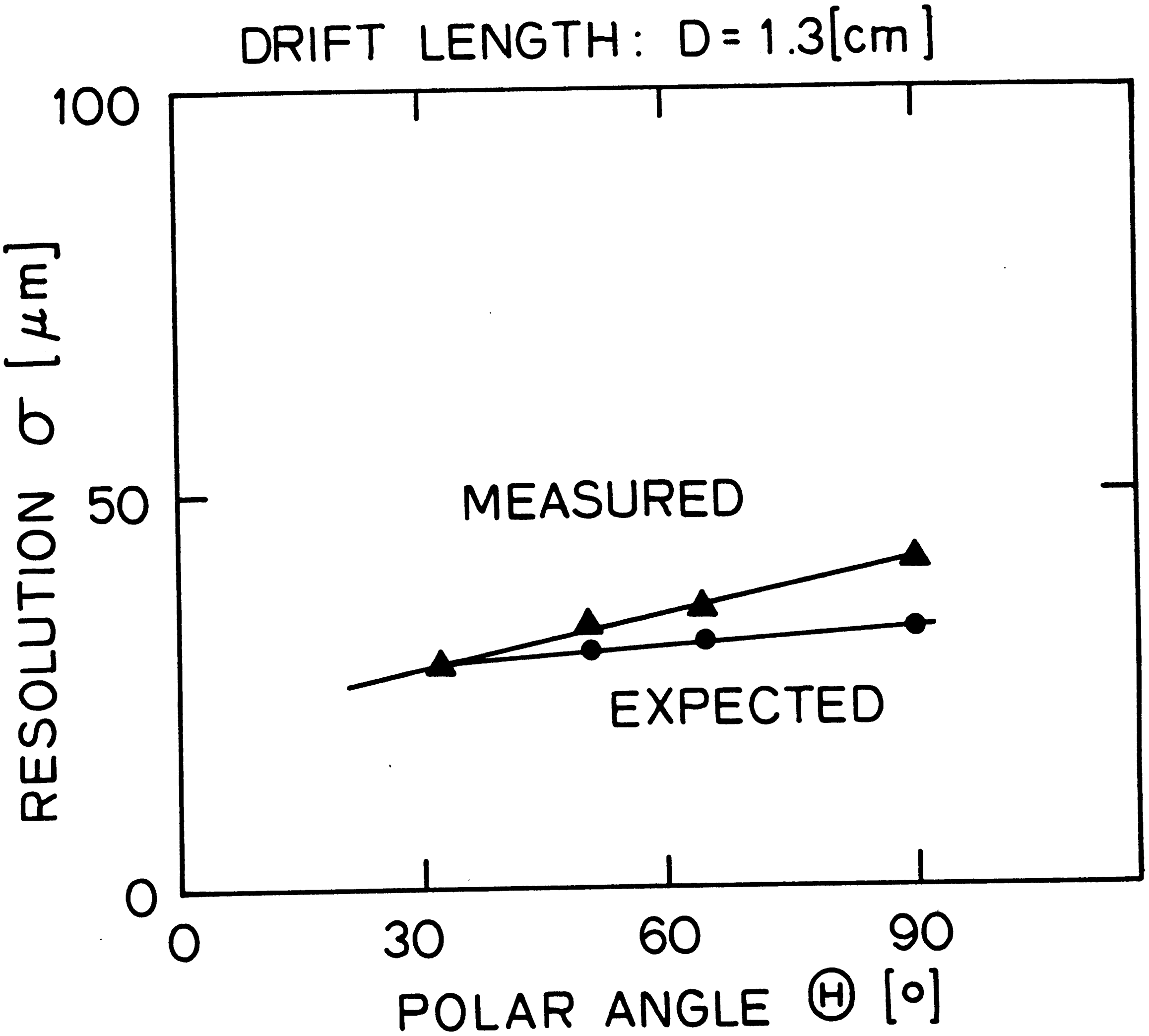
DRIFT LENGTH: D = 1.3[cm]
100
50
0
RESOLUTION σ [μm]
MEASURED
EXPECTED
0
30
60
90
POLAR ANGLE Θ [°]

FIG. 8

MARK_J TEC

VOLOUME TEC219 RUN 10360 EVENT 218 EVENT_MKJ 219

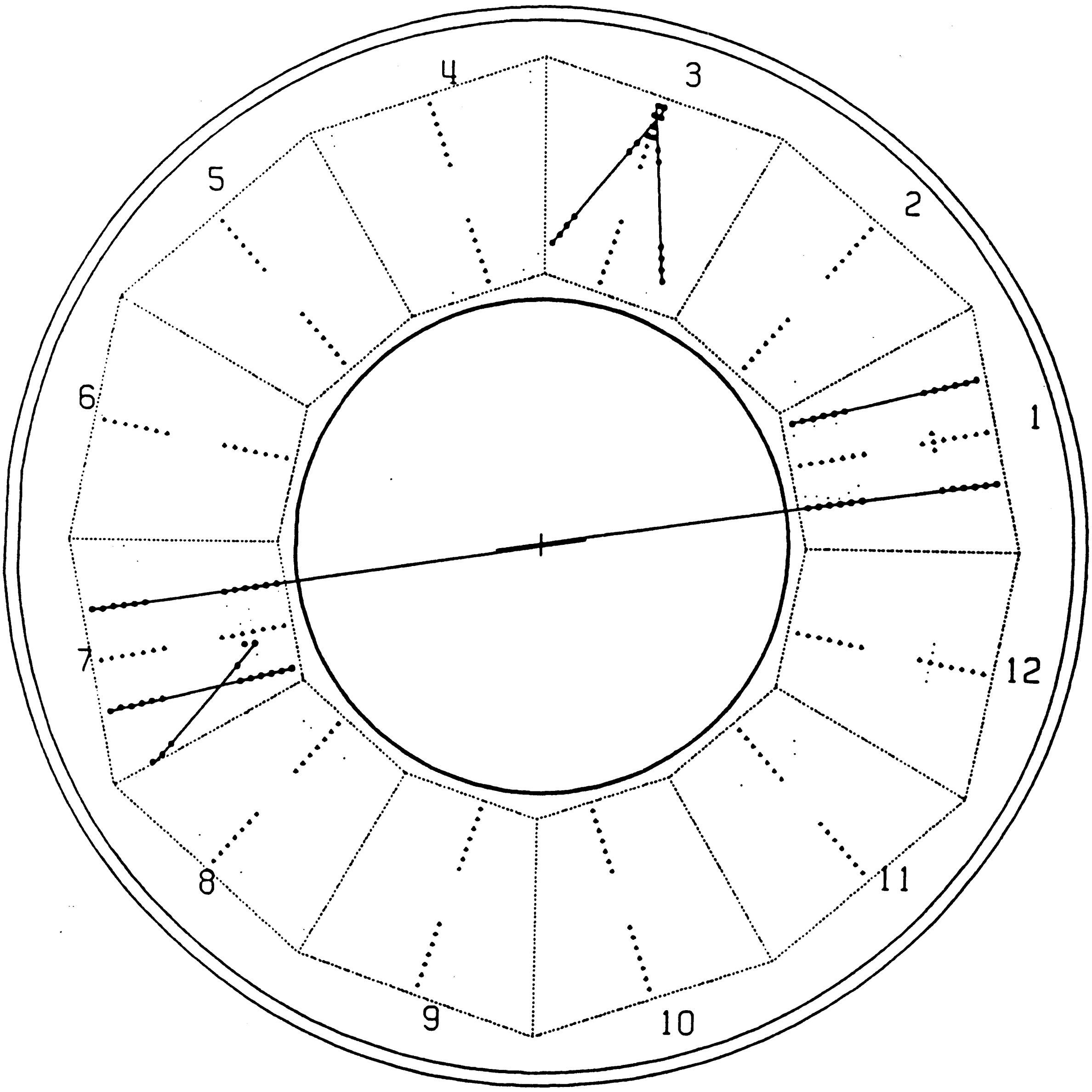

FIG. 9

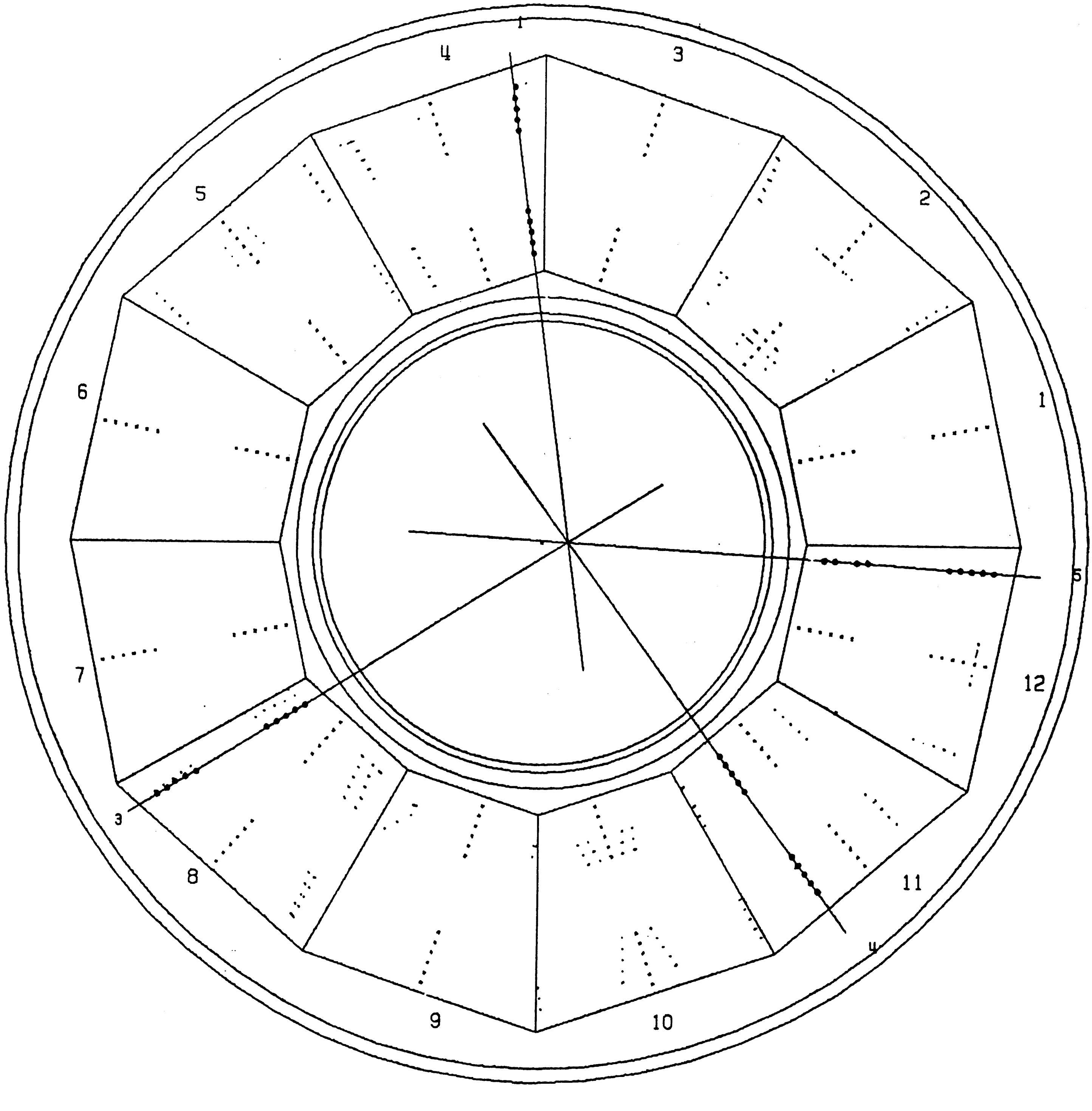

FIG. 10

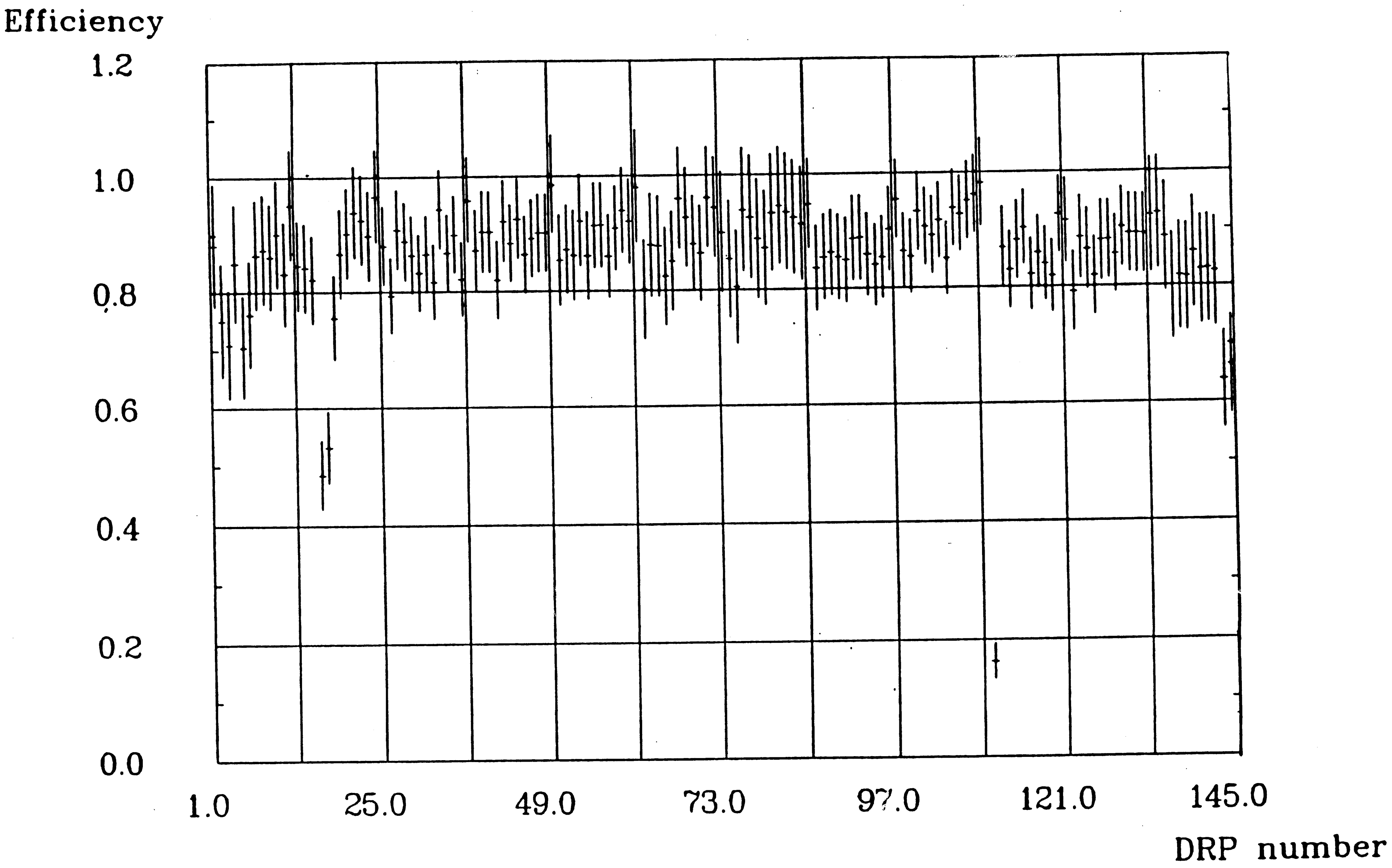
Efficiency
1.2
1.0
0.8
0.6
0.4
0.2
0.0
1.0
25.0
49.0
73.0
97.0
121.0
145.0
DRP number

FIG. 11

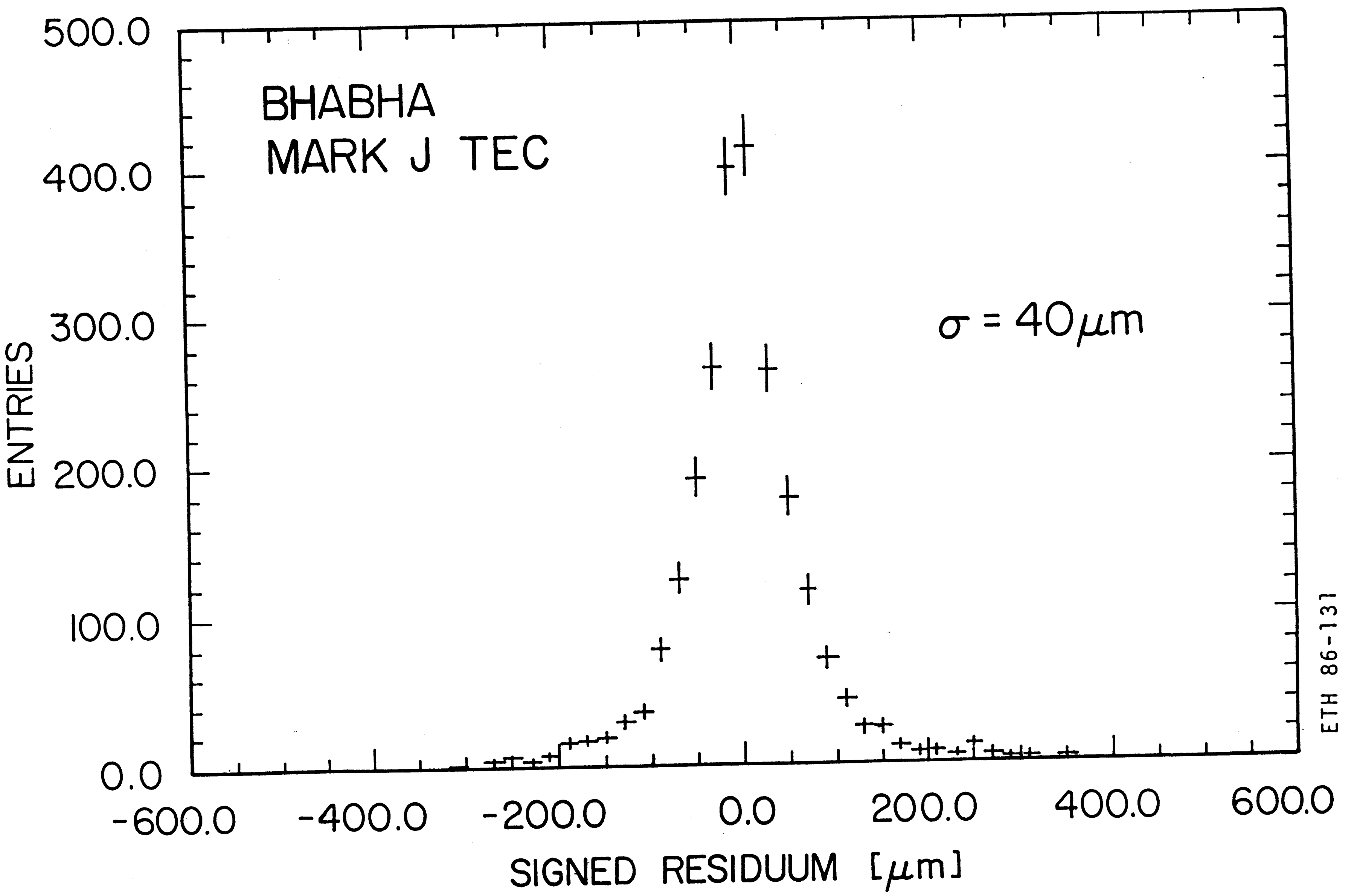
BHABHA
MARK J TEC
σ = 40μm
ENTRIES
500.0
400.0
300.0
200.0
100.0
0.0
-600.0
-400.0
-200.0
0.0
200.0
400.0
600.0
SIGNED RESIDUUM [μm]
ETH 86-131

FIG. 12

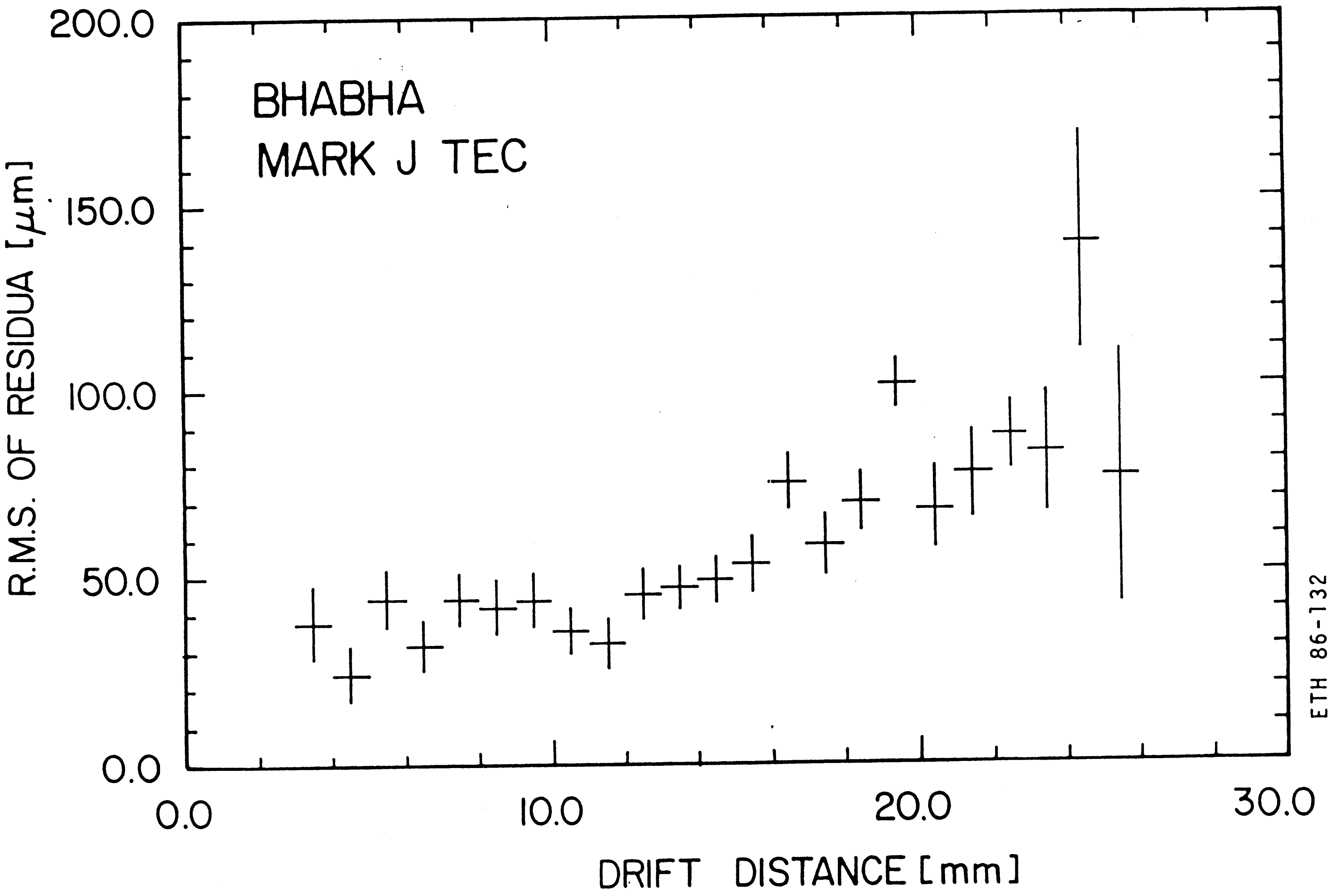
BHABHA
MARK J TEC
R.M.S. OF RESIDUA [μm]
200.0
150.0
100.0
50.0
0.0
0.0
10.0
20.0
30.0
DRIFT DISTANCE [mm]
ETH 86-132

FIG. 13